Engineering Structures 145 (2017) 381–391

Contents lists available at ScienceDirect

Engineering Structures

journal homepage: www.elsevier.com/locate/engstruct

Lifetime reliability-based optimization of post-tensioned box-girder bridges

Tatiana García-Segura [a,*], Víctor Yepes [a], Dan M. Frangopol [b], David Y. Yang [c]

[a] Institute of Concrete Science and Technology (ICITECH), Universitat Politècnica de València, 46022 Valencia, Spain
[b] Department of Civil and Environmental Engineering, Engineering Research Center for Advanced Technology for Large Structural Systems (ATLSS Center), Lehigh University, 117 ATLSS Dr., Bethlehem, PA 18015-4729, USA
[c] Department of Civil and Environmental Engineering, The Hong Kong Polytechnic University, Hung Hom, Hong Kong, China

ARTICLE INFO

Article history:
Received 29 July 2016
Revised 7 March 2017
Accepted 8 May 2017
Available online 23 May 2017

Keywords:
Corrosion
Lifetime performance
Sustainability
Post-tensioned concrete
Box-girder bridges

ABSTRACT

This paper presents a lifetime reliability-based approach for the optimization of post-tensioned concrete box-girder bridges under corrosion attack. The proposed approach is illustrated by determining the optimal life-cycle cost and CO_2 emissions of several initial designs of post-tensioned box-girder bridges with different objectives, i.e. the lowest initial costs, the longest corrosion initiation time, or the maximum safety. The study was conducted in two steps. Firstly, the Pareto set presents initial designs considering the cross-section geometry, the concrete strength, the reinforcing steel and the prestressing steel. Secondly, the maintenance optimization was conducted with the proposed method, aimed at minimizing the economic, environmental and societal impacts of the bridge while satisfying the reliability target during its life-span. Effective maintenance is able to extend the service life of the bridge with the minimum cost and CO_2 emissions. It is indicated that a durability-conscious initial design is particularly beneficial for life-cycle performance. Besides, the emphasis on the initial design can also have an effect on the life-cycle performance of bridges. It is found that designs with longer corrosion initiation time are associated with lower life-cycle cost, especially when using concrete of higher strength. Findings from the current paper also indicate that optimal maintenance strategies are more likely to be those with fewer maintenance actions that repair all deteriorating structures simultaneously.

1. Introduction

Sustainable development requires a balance among the economic, environmental and societal pillars. In addition, the Brundtland Report proposes a long-term vision to maintain the resources necessary to provide future needs [1]. This objective has been applied to the civil engineering field in different lines of research. Some researches deal with design optimizations aimed to achieve the maximum benefit from the minimum resources [2–5]. Environmental concern has led to the incorporation of CO_2 emissions and energy consumptions as important criteria [6–10]. Moreover, environmental effects from other industries during the civil engineering activities have also been studied in order to reduce the total CO_2 emissions [11,12]. Other studies focus on the life-cycle perspective. Sarma and Adeli [13] presented a review on cost optimization of concrete structures and stated that the focus of further research should switch from initial cost optimization to life-cycle cost optimization. This has led to an increased number of studies on life-cycle performance of structures [14–17], aiming at optimizing the maintenance cost of structures. Frangopol and Soliman [18] pointed out that maintenance actions must be effectively planned throughout the life-cycle of structures to achieve the maximum possible life-cycle benefits under budget constraints.

A major portion of the life-cycle cost of long-span coastal bridges is attributed to the maintenance of corroded components [19]. A maintenance action can delay the damage propagation or reduce the degree of damage, and consequently, extend the service life of a deteriorating structure [20]. Neves and Frangopol [21] mentioned that including condition states alone is not enough to reflect the safety and serviceability of a bridge. Thus, both condition and safety levels have been used as objectives in maintenance optimization [22–24]. Later, Dong et al. [25] considered the environmental and societal aspects of maintenance actions. Sabatino et al. [26] used multi-attribute utility theory to assess various

* Corresponding author.
E-mail addresses: tagarse@cam.upv.es (T. García-Segura), vyepesp@cst.upv.es (V. Yepes), dan.frangopol@lehigh.edu (D.M. Frangopol), ynyang1988@gmail.com (D.Y. Yang).

http://dx.doi.org/10.1016/j.engstruct.2017.05.013
0141-0296/

aspects of structural sustainability considering risks associated with bridge failure and risk attitudes of decision makers. Penadés-Plà et al. [27] reviewed the sustainable criteria used for decision-making at each life-cycle phase of a bridge.

The performance of a structure is affected by several uncertainties. Among these, uncertainties in load effects, material properties and damage occurrence and propagation should be highlighted [28]. Many design codes, including the Eurocode, have adopted the partial safety factors to take into account the uncertainties arising from geometry, material properties, load effects, and design models. During the planning of maintenance actions, stakeholders should also be well aware of the uncertainties involved in the deterioration process and potential inspections/interventions [17]. A proper consideration of uncertainties can lead to significant economic benefits for both initial design and life-cycle performance [29].

This paper presents a lifetime reliability-based approach for the optimization of post-tensioned concrete (PTC) box-girder road bridges through two steps. Firstly, the study relies on a novel multi-objective optimization technique developed by García-Segura et al. [30] to arrive at a set of optimum initial bridge solutions considering initial cost, overall safety factor and corrosion initiation time, constrained by the requirements of the design code. Secondly, maintenance optimization is conducted with respect to a design service life of 150 years to determine the optimal maintenance actions in terms of maintenance costs and environmental impacts. The maintenance actions considered in the study can delay the damage propagation, which in turn extends the bridge service life. The economic, environmental and societal impacts are examined. During the maintenance optimization, the societal impact due to traffic disruptions is associated with either economic costs or CO_2 emissions based on existing studies [25]. The comparison of life-cycle cost and CO_2 emissions among the initial designs under consideration provides guidance for designing sustainable PTC box-girder road bridges in a coastal zone.

2. Pareto front of optimal bridge designs

The paper studies the design of a PTC box-girder road bridge located in a coastal region. The initial designs under consideration are selected from a set of alternative tradeoff solutions located on a Pareto front associated with three objectives: initial cost, overall safety factor, and corrosion initiation time. The determination of these objectives are described in detail in the following sections. Bridge designs are obtained from the following optimization scheme:

Given

A PTC box-girder road bridge with a width of 11.8 m and three continuous spans of 35.2, 44 and 35.2 m.

Goal

Find the optimal bridge design of a PTC box-girder described by 34 variables regarding the geometry, the reinforcing and prestressing steel, and the concrete grade. Fig. 1 shows the geometric variables of the bridge section as well as the longitudinal and transverse reinforcement. The diameters of rebars are denoted as $LR_{1\text{-}10}$ and $TR_{1\text{-}8}$ for longitudinal and transverse steel respectively. Note that the deck is divided into two zones: pier zones (L/5 on both sides of the piers) and girder zones (the rest of the span). In pier zones, rebars with diameters of LR_7 and LR_9 are provided as extra reinforcement in the top and bottom slab, respectively. In the girder zones, rebars with diameters of LR_8 and LR_{10} are extra reinforcement in the top and bottom slab, respectively. Regarding transverse steel, an extra reinforcement with diameter of TR'_4 is placed at the same position as TR_4 and covers the support zone (L/5 on both sides of all supports). In all zones, TR_9 is fixed at 12 mm. The number of longitudinal rebars per meter (N_{LR}) as well as the spacing of the transverse reinforcement (S_{TR}) does not vary along the longitudinal axis of the bridge section. The post-tensioning steel is formed by strands symmetrically distributed through the webs. The variables associated with post-tensioning steel are the distance from the pier section to the point of inflection as a ratio of the span length (L_{pi}), the eccentricity in the external spans as a ratio of half of the bridge depth (e_p), and the number of strand (N_S). The eccentricity in the midspan of the central span and in the supports is set to be the maximum value allowed in the design code. The prestressing force in each strand is fixed as 195.52 kN. Finally, the last variable under consideration is the concrete grade (f_{ck}). All these 34 variables should be selected to simultaneously optimize the following objectives:

- Minimize the initial cost of material production and construction
- Maximize the overall safety factor with respect to the ultimate limit states
- Maximize the corrosion initiation time

Subject to

The requirements related to the ultimate and serviceability limit states described in Fomento [31,32], are based on the Eurocodes 1 and 2 [33,34]. The ultimate limit states considered herein include shear, shear between web and flanges, punching shear, flexure and torsion, whereas the serviceability limit states examined herein include deflection and cracking. In addition, the codes require the decompression of prestressing strands in coastal environments, i.e. decompression must not occur in the concrete located 100 mm above and under the strands [33]. For serviceability limit states associated with bridges, the codes also limit the instantaneous and time-dependent deflection due to precamber effects to 1/1400th of the main span length under the characteristic combination [31], and the deflection associated with the frequent value for the live loads is limited to 1/1000th of the main span length [32]. The geometrical and constructability requirements are also examined according to the codes. Load effects take into account of the traffic loads [32], the self-weight of parapets (5 kN/m) and asphalt (24 kN/m^3), the thermal gradient [32], the

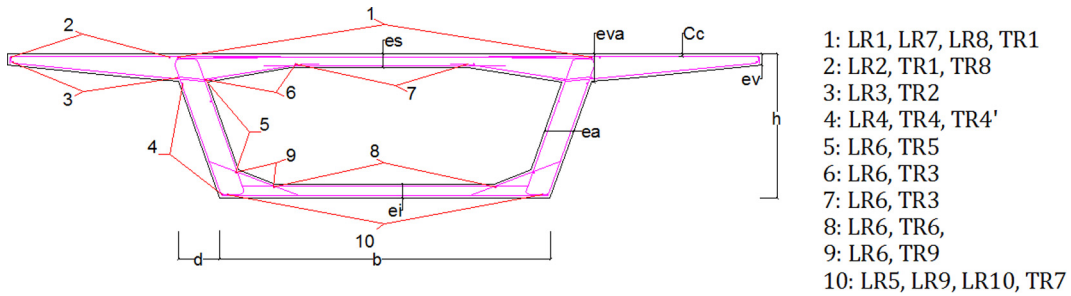

Fig. 1. Variables regarding geometry and reinforcing steel of the PTC box-girder road bridge.

prestressing steel effect and the relative settlement of each support (5 mm).

2.1. Objective 1: initial cost

The initial cost (C_{ini}) is obtained according to Eq. (1). Each unit cost (concrete (C_{co}), reinforcing steel (C_{rs}), prestressing steel (C_{ps}) and formwork (C_f)) is multiplied by the respective measurements (volume of concrete (V_{co}), the weight of reinforcement steel (W_{rs}), the weight of prestressing steel (W_{ps}) and the area of the formwork (A_f)). The unit costs for the materials are evaluated as the cost of material production, transport and placement. The cost of material production includes the raw material extraction, manufacture and transport. Table 1 summarizes the unit costs used in the optimization. More details can be found in Garcia-Segura et al. [6].

$$C_{ini} = C_{co} \cdot V_{co} + C_{rs} \cdot W_{rs} + C_{ps} \cdot W_{ps} + C_f \cdot A_f \quad (1)$$

2.2. Objective 2: overall safety factor

Eq. (2) evaluates the overall safety factor (S) as the minimum coefficient (γ_j) of the torsion, flexure, transverse flexure and shear limit states. The coefficient γ_j is defined as the ratio of the design value of the ultimate resistance to the design value of ultimate load effects. For the determination of these design values, partial safety factors should be considered as proposed by the codes [31,32]. Therefore, a safety coefficient of 1 indicates strict compliance with the codes.

$$S(\vec{x}) = Minimum\,\gamma_j(\vec{x}) \quad (2)$$

2.3. Objective 3: corrosion initiation time

For structures in a coastal environment, the corrosion initiation time (t_{corr}) corresponds to the time when the chloride concentration on the surface of reinforcing steel exceeds a critical threshold value (C_r). At time t, the chloride content at a distance x from the concrete outer surface is calculated based on Fick's second law (see Eq. (3)).

$$C(x,t) = C_o\left[1 - \mathrm{erf}\left(\frac{x}{2\sqrt{tD}}\right)\right] \quad (3)$$

where D is the apparent diffusion coefficient; C_o is the chloride concentration on the surface. The current study considers the uncertainties related to the apparent diffusion coefficient, chloride concentration on the surface, concrete cover, and the threshold value of chloride content. The apparent diffusion coefficient reflects the concrete permeability. Eq. (4) is used herein to determine the diffusion coefficient [35,36]:

$$D = D_{H_2O}0.15 \cdot \frac{1 + \rho_c \frac{w}{c}}{1 + \rho_c \frac{w}{c} + \frac{\rho_c a}{\rho_a c}}\left(\frac{\rho_c \frac{w}{c} - 0.85}{1 + \rho_c \frac{w}{c}}\right)^3 \quad (4)$$

where D_{H20} is the chloride diffusion coefficient in an infinite solution (=1.6 × 10^{-5} cm^2/s for NaCl); ρ_c is the mass density of cement (considered to be 3.16 g/cm^3); ρ_a is the mass density of aggregates (considered to be 2.6 g/cm^3); a/c is the aggregate-to-cement ratio; and w/c is the water-cement ratio. The values of aggregate-to-cement ratio and water-cement ratio are shown in Table 3 according to the concrete grades. The parameters of the random variables associated with the corrosion initiation are summarized in Table 2 [35]. It should be noted that the coefficient of variation of C_o is assumed herein as 0.3 due to the reduced variability of the surface chloride content in a particular bridge compared to a group of bridges considered in [37]. The mean value of the surface chloride content corresponds to a distance of 1000 m from the coast [37].

Table 1
Unit costs and CO_2 emissions.

Unit measurements	Cost (€)	CO_2 emission (kg)
m^2 of formwork	33.81	2.08
kg of steel (B-500-S)	1.16	3.03
kg of prestressing steel (Y1860-S7)	3.40	5.64
m^3 of concrete 35 MPa	104.57	321.92
m^3 of concrete 40 MPa	109.33	338.90
m^3 of concrete 45 MPa	114.10	355.88
m^3 of concrete 50 MPa	118.87	372.86
m^3 of concrete 55 MPa	123.64	389.84
m^3 of concrete 60 MPa	128.41	406.82
m^3 of concrete 70 MPa	137.95	440.78
m^3 of concrete 80 MPa	147.49	474.74
m^3 of concrete 90 MPa	157.02	508.70
m^3 of concrete 100 MPa	166.56	542.66

Table 2
Parameters of the random variables associated with corrosion.

Random variables	Probabilistic distributions
Model error (D)	Normal (μ = 1, COV = 0.2)
C_o	Lognormal (μ = 2.95, COV = 0.3)
C_r	Uniform (0.6–1.2)
Model error for i_{corr}	Uniform (μ = 1, COV = 0.2)
Cover	Normal ($\mu = c_c$, COV = 0.25)

Table 3
Aggregate-to-cement ratio and water-cement ratio of different concrete grades.

Concrete grade	a/c	w/c
35 MPa	6.45	0.54
40 MPa	6.03	0.5
45 MPa	5.47	0.45
50 MPa	4.66	0.4
55 MPa	3.92	0.35
60 MPa	3.64	0.33
70 MPa	3.56	0.31
80 MPa	3.55	0.3
90 MPa	3.52	0.3
100 MPa	3.22	0.3

3. Maintenance optimization

Maintenance optimization seeks sustainable maintenance actions that maintain the bridge performance requirements during its life-span. For bridges in coastal zones, deterioration is mainly caused by chloride-induced steel corrosion. Long-term effects of prestressing tendons, such as loss of prestress and deflection, are considered in the initial design phase. The degradation process due to chloride-induced corrosion is formulated as a reduction of the reinforcing steel area. Consequently, the structural safety is reduced. A lifetimereliability-based approach is used to evaluate the structural performance and to satisfy the annual reliability target index of 4.7, as proposed in the Eurocode [38]. Maintenance actions are applied to keep the minimum reliability index above the target level during the prescribed service life (150 years). The optimization variables define the maintenance schedule in each cross-section (see Fig. 2). The maintenance optimization considers the three pillars of sustainability, i.e. economic, environmental and societal impacts. The economic impact of maintenance actions derives from the material and construction costs of maintenance actions. The environmental impact considers the CO_2 emissions due to the materials and construction activities. The societal impact is due to the traffic disruptions during maintenance actions.

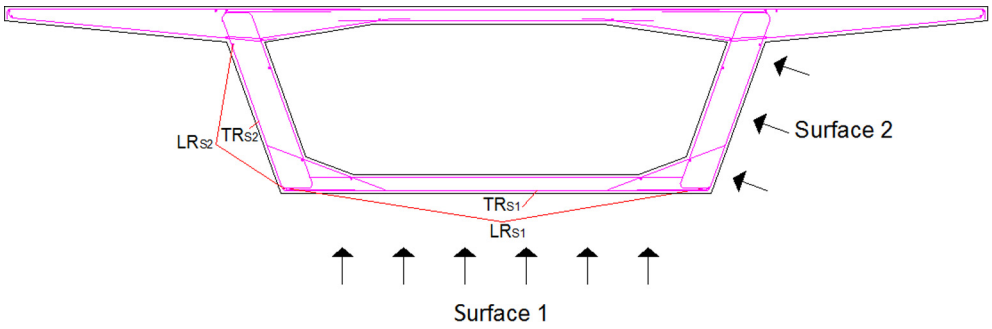

Fig. 2. Surfaces affected by corrosion propagation.

In the current study, the societal impact is merged into the economic and environmental consequences respectively during the optimization process. Therefore, two single objective optimizations are made considering economic and environmental consequences as objectives, respectively. A harmony search algorithm is used for the single objective optimization of costs and CO_2 emissions due to maintenance actions. The optimization problem is formulated as follows:

Given

The bridge design from the previous initial design optimization, as well as the effect of concrete repair on the chloride-induced corrosion.

Goal

Find the optimal time of the first maintenance application and the number of applications on surface 1 (t_1 and n_1) and surface 2 (t_2 and n_2), as shown in Fig. 2, so that:

- The costs of maintenance actions, which include the direct and indirect maintenance costs, are minimized

  OR

- The CO_2 emissions due to maintenance actions, which are caused by the direct and indirect consequences, are minimized

Subject to

The minimum annual target reliability index of 4.7. Therefore, the annual reliability index of the bridge must be at least this value during the entire service life.

3.1. Deterioration process

The deterioration analysis is carried out considering uniform corrosion of the reinforcing steel. The corrosion rate is expressed as a time-dependent variable based on the corrosion initiation time and the corrosion rate at the start of corrosion propagation ($i_{corr}(1)$), as indicated below [35]:

$$i_{corr}(t) = i_{corr}(1) \cdot 0.85 \cdot (t - t_{corr})^{-0.29} \tag{5}$$

$$i_{corr}(1) = \frac{37.8(1 - w/c)^{-1.64}}{C_c} \tag{6}$$

$$D_b = D_{b0} - 2 \cdot \int_{T_i}^{t} 0.0116 \cdot i_{corr}(t)dt \tag{7}$$

The reinforcement diameter decreases after t_{corr} according to the assumption of uniform corrosion. Note that 1 μA/cm^2 is equivalent to 0.0116 mm/year. It is considered herein that the pavement thickness increases the cover of the top slab. Therefore, the reinforcement located near this surface is not critical. Hence, it is not considered in the deterioration analysis. Likewise, the prestressing tendons are considered to be immune from corrosion, since they are located sufficiently far away from the surface. As a result, the corrosion propagation affects mainly the longitudinal and transverse reinforcement beneath surfaces 1 and 2 (LR_{S1}, LT_{S1}, LR_{S2}, LT_{S2}). Table 4 summarizes the limit states affected by the reinforcing steel corrosion.

3.2. Lifetime performance

The lifetime performance of the bridge is evaluated by reliability indices (β) computed using the First Order Second Moment (FOSM) method as follows:

$$p_f = P_r[(R - S) < 0] \tag{8}$$

$$\beta = -\Phi^{-1}(p_f) \tag{9}$$

$$\beta = \frac{\bar{R} - \bar{S}}{\sqrt{\sigma_R^2 + \sigma_S^2}} \tag{10}$$

where p_f is the probability of failure; Φ^{-1} is the inverse standard normal cumulative distribution function; R is the generalized structural resistance, S is the generalized action effect; $\bar{R}$ and $\bar{S}$ are mean values of R and S respectively; and σ_R and σ_S are the standard deviations of R and S. Table 5 shows the statistical parameters for material properties and loading variables. The uncertainties inherent in concrete and steel properties are described by a normal distribution [39]. Mean values are obtained considering that characteristic values correspond to the 5th percentile of material strength distributions. The generalized structural resistance is evaluated following the structural code [31]. It should be noted that no partial safety factors are considered for the evaluation of the resistance.

Regarding the generalized action effects, the mean value of permanent load effects can be determined by the coefficient of variation (COV) and the characteristic value [40]. The variable loads are represented by Gumbel distributions. The relation between the characteristic value and the mean annual extreme can be obtained as follows:

$$Q_K = \mu \cdot [1 - V\frac{\sqrt{6}}{\pi}[0.577 + ln(-\ln(1 - p))]] \tag{11}$$

where Q_K is the characteristic value; μ is the mean annual extreme; V is the coefficient of variation and p is the probability of being exceeded. The characteristic values for the temperature-gradient effects (hereafter termed as the temperature load) and traffic load effects are obtained from Fomento [32] and Eurocode [34,41]. Regarding the temperature load, the characteristic value corresponds to an annual probability of being exceeded of 0.02 [41], i.e. $p = 0.02$ in Eq. (11). The coefficient of variation of the temperature load is 40% based on available measurement data of

Table 4
Limit states and reinforcement affected by corrosion.

Surface (see Fig. 2)	Reinforcement diameter	Limit state
1	LR_{S1}	Torsion Flexure
	TR_{S1}	Transverse flexure Torsion
2	LR_{S2}	Torsion
	TR_{S2}	Transverse flexure Torsion Shear

Table 5
Statistical parameters for material properties and loading variables.

Random Variables	Model type
Concrete compressive strength	Normal (COV = 0.18)
Concrete tension strength	Normal (COV = 0.18)
Reinforcing steel strength	Normal (COV = 0.098)
Prestressing steel strength	Normal (COV = 0.025)
Permanent	Normal (COV = 0.1)
Gradient	Gumbel (COV = 0.4)
Traffic load	Gumbel (COV = 0.15)

existing bridges [42,43]. For the traffic load, the annual characteristic value with a probability of exceedance of 5% is 90% of the 50-year characteristic value [44]. The coefficient of variation for traffic loads is 0.15 [45,46].

3.3. Design variables

This study considers concrete repair as bridge maintenance actions. It includes the removal of old concrete cover and its replacement. As the concrete cover regains its initial state, the degradation of the structural capacity is halted for a period equal to the corrosion initiation time of the new cover. The new corrosion initiation time (t_{corr2}) depends on the new water cement ratio and the thickness of the cover. A water cement ratio of 0.4 and a thickness of 30 mm are considered. The new cover has a different corrosion rate. Consequently, the structure after concrete repair deteriorates at a different rate. The design variables of maintenance optimization include the time of the first application and the number of applications on surface 1 (t_1 and n_1) and surface 2 (t_2 and n_2), respectively. The time interval between applications is considered constant. The time-dependent evolution of the reliability index depends on the values of design variables.

3.4. Optimization algorithm

This paper uses a modified harmony search algorithm to conduct the single objective optimization of maintenance actions. Harmony search, proposed by Geem et al. [47], establishes an analogy between optimization and the tuning for the best musical harmony. The following steps explain the algorithm procedure:

Step 1 – Assignment of the algorithm parameters. The algorithm parameters are: harmony memory size (HMS), harmony memory considering rate (HMCR), pitch adjusting rate (PAR) and the maximum number of improvisations without improvement (IWI).

Step 2 – Memory initialization. A harmony memory matrix (HM) is filled with random values of the design variable pool. The harmony vectors or solutions must be feasible considering the exerted constraints.

Step 3 – Improvisation of a new solution. A new harmony vector is improvised in each iteration. The algorithm selects the values of the variables by a selection either from design variable pool or from HM. The new harmony vectors are improvised according to three procedures:

Option 1- Random selection. The probability of choosing the values of the variables from the design variable pools is 1-HMCR.
Option 2- Memory consideration. The probability of choosing the values of the variables from the HM is HMCR.
Option 2.1- Pitch adjustment. After the memory consideration, the probability of modifying the value one position up or down is PAR.

Step 4 – HM update. The new solution replaces the worst harmony if its objective function value improves the worst one.

Step 5 – Termination criterion. The optimization process returns to Steps 3 if the iterations without improving the best harmony reaches IWI.

In conventional HS, memory consideration chooses each variable from a random HM solution. García-Segura et al. [30] showed that combining solutions is less effective than taking only one solution and perturbing some members. According to that, new solutions are the result of random selection, memory consideration to one random solution of HM, and pitch adjustment. On that basis, this study improves the algorithm performance by selecting design variables merely from two HM solutions. In this case, memory consideration chooses two random solutions in each iteration to make the maintenance of surface 1 and 2 independent. Two variables, which refer to the maintenance of surface 1, are chosen from one random selection from the HM and two more variables, regarding surface 2, are taken from another random selection. The parameters are selected according to the Design of Experiments methodology [6]. The calibration process suggested HMS = 10, HMCR = 0.9, PAR = 0.4 and IWI = 50.

3.5. Sustainability criteria

3.5.1. Economic impact

Economic impact (C_{ms}) of maintenance actions results from the direct cost of maintenance applications. To transfer future costs of maintenance actions (t) to the present values, the time value of money is considered through a discount rate (v). The maintenance cost is calculated for surfaces 1 (C_{mS1}) and 2 (C_{mS2}) as follows:

$$C_{ms} = \sum_{j=1}^{Nms1} \frac{C_{ms1j}}{(1+v)^{t_j}} + \sum_{j=1}^{Nms2} \frac{C_{ms2j}}{(1+v)^{t_j}} \tag{12}$$

where N_{mS1} and N_{mS2} are the total numbers of maintenance actions over each surface, respectively. For concrete repair, water blasting is required to remove the old concrete cover. In addition, an adhesion coating is applied to prepare a proper surface for new concrete cover. Finally, repair mortar is cast to form the new cover. All these activities are carried out by a truck mounted platform. As a result, the following equation is used to calculate maintenance costs, i.e. C_{ms1} and C_{ms2} in Eq. (12).

$$C_{msij} = ((C_{wb} + C_{rm}) \cdot V_{csi} + (C_{bc} + C_{tp}) \cdot A_{si}) \tag{13}$$

where C_{wb} is the cost of water blasting, C_{rm} is the cost of the repair mortar application, C_{bc} is the cost of the bonding coat application, C_{tp} is the cost of the truck mounted platform and V_{csi} and A_{si} are the volume and the area of concrete replaced on surface i. The thickness of the removed cover is considered to be equal to the old concrete cover thickness plus rebar diameter. Table 6 summarizes the unit costs used for the preceding evaluation [25,48–50]. Note that lognormal distributions (LN) with coefficients of variation of 0.2 are also considered for these unit costs.

Table 6
Costs and emissions associated with the direct and indirect maintenance.

Mean cost	Mean CO_2 emission	COV	Distribution type
C_{wb} = 11.5 (€/m^2/cm) [49]	E_{wb} = 0.91 (kg/m^2/cm) [48]	0.2	LN
C_{bc} = 16.41 (€/m^2) [48]	E_{bc} = 15.85 (kg/m^2) [48]	0.2	LN
C_{rm} = 43.28 (€/m^2/cm) [50]	E_{rm} = 25.5 (kg/m^2/cm) [48]	0.2	LN
C_{tp} = 53.71 (€/m^2) [48]	E_{tp} = 142.09 (kg/m^2) [48]	0.2	LN
$C_{run,cars}$ = 0.07 (€/km) [25]	$E_{run,cars}$ = 0.22 (kg/km) [25]	0.2	LN
$C_{run,truck}$ = 0.34 (€/km) [25]	$E_{run,truck}$ = 0.56 (kg/km) [25]	0.2	LN
C_{wage} = 20.77 (€/h) [25]		0.15	LN
C_{driver} = 24.54 (€/h) [25]		0.15	LN
C_{cargo} = 3.64 (€/h) [25]		0.2	LN

3.5.2. Environmental impact

The environmental impact of maintenance actions (E_{ms}) includes the CO_2 emitted during the maintenance actions. The CO_2 emissions produced during a maintenance action, for surfaces 1 (E_{mS1}) and 2 (E_{mS2}), respectively, are obtained as an aggregation of emissions due to water blasting (E_{wb}), repair mortar applications (E_{rm}), bond coating applications (E_{bc}) and truck platform mounting (E_{tp}), as shown in Eqs. (14) and (15).

$$E_{ms} = \sum_{j=1}^{Nms1} E_{ms1j} + \sum_{j=1}^{Nms2} E_{ms2j} \tag{14}$$

$$E_{msij} = ((E_{wb} + E_{rm}) \cdot V_{csi} + (E_{bc} + E_{tp}) \cdot A_{si}) \tag{15}$$

The maintenance unit emissions can be found in the BEDEC database [48].

3.5.3. Societal impact

The societal impact arises from the traffic disruptions during maintenance actions. This study considers societal impact only once if the interval between two maintenance actions is less than one year. To quantify the loss associated with traffic disruptions, the societal impact of maintenance actions is converted to economic loss or extra emissions depending on which objective is being considered. The cost of the societal impact (C_s) is computed based on the running cost (C_{run}) due to detours and time loss (C_{time}) due to increased travel time. Likewise, extra CO_2 emissions (E_s) are induced by running on detours (E_{run}). The societal impact in terms of cost and CO_2 emission can be determined by the following equations [25]:

$$C_{s=}C_{run} + C_{time} \tag{16}$$

$$C_{run} = \sum_{i=1}^{Nm} \left[C_{run,cars}\left(1 - \frac{T_{truck}}{100}\right) + C_{run,truck}\left(\frac{T_{truck}}{100}\right) \right] \frac{L_{detour} T_{detour} A_{DT}}{(1+v)^t} \tag{17}$$

$$C_{time} = \sum_{i=1}^{Nm} \left[C_{wage} O_{cars}\left(1 - \frac{T_{truck}}{100}\right) + (C_{driver} O_{truck} + C_{cargo}) \frac{T_{truck}}{100} \right] \frac{L_{detour} T_{detour} A_{DT}/S}{(1+v)^t} \tag{18}$$

$$E_S = E_{run} = \sum_{i=1}^{Nm} \left[E_{run,cars}\left(1 - \frac{T_{truck}}{100}\right) + E_{run,truck}\left(\frac{T_{truck}}{100}\right) \right] L_{detour} T_{detour} A_{DT} \tag{19}$$

where N_m is the number of traffic disruptions; $C_{run,cars}$ and $C_{run,truck}$ are the unit cost of running cars and trucks, respectively; T_{truck} is the average daily truck traffic ratio; A_{DT} is the average daily traffic; L_{detour} is the detour length; and T_{detour} is the detour time; C_{wage} is the wage compensation for car drivers; C_{driver} is the truck driver compensation; C_{cargo} is the value of a cargo; O_{cars} is the average vehicle occupancies for cars; O_{truck} is the average vehicle occupancies for trucks; S is the speed on detours; regarding the running emissions, $E_{run,cars}$ and $E_{run,truck}$ are CO_2 emissions for running cars and trucks respectively. Table 7 summarizes the parameters considered for the evaluation of the societal impact [25].

Table 7
Traffic conditions during the detour [25].

Unit measurements	Mean value	COV	Distribution type
T_{truck} (%)	12	0.2	LN
A_{DT} (veh/day)	8500	–	Deterministic
L_{detour} (km)	2.9	–	Deterministic
T_{detour} (day)	7	–	Deterministic
S (km/h)	50	0.15	LN
O_{cars}	1.5	0.15	LN
O_{truck}	1.05	0.15	LN
v (%)	2	–	Deterministic

The costs and emissions associated with the societal impact are added to the economic and environmental impacts respectively to obtain the total cost (TC_{ms}) and CO_2 emissions (TE_{ms}) due to maintenance actions:

$$TC_{ms} = C_{ms} + C_s \tag{20}$$

$$TE_{ms} = E_{ms} + E_s \tag{21}$$

4. Life-cycle performance of box-girder road bridges

By combining the initial cost and emissions from Section 2 and those due to maintenance actions in Section 3, one can evaluate the life-cycle cost and emissions of bridge designs under consideration. Fig. 3 shows the flowchart followed by the current study for the determination of life-cycle cost and emissions. Firstly, the maintenance optimization considers the economic, environmental and societal impacts of maintenance. The initial cost and emissions are not considered since the optimal maintenance solutions do not depend on these terms. Then, for the life-cycle evaluation, the initial costs, which include material and construction costs obtained from Section 2, are considered. Note that construction costs are incurred at year zero, i.e. present values. For the life-cycle emissions, the CO_2 emissions with respect to the materials and construction can be determined similarly by substituting the unit costs in Eq. (1) with unit emissions:

$$E_{ini} = E_{co} \cdot V_{co} + E_{rs} \cdot W_{rs} + E_{ps} \cdot W_{ps} + E_f \cdot A_f \tag{22}$$

where the CO_2 emissions associated to concrete (E_{co}), reinforcing steel (E_{rs}), prestressing steel (E_{ps}) and formwork (E_f) are obtained from the BEDEC database [48]. Table 1 shows these values.

The initial cost and emissions are added to the maintenance cost and emissions in order to obtain the life-cycle cost (TC) and CO_2 emissions (TE):

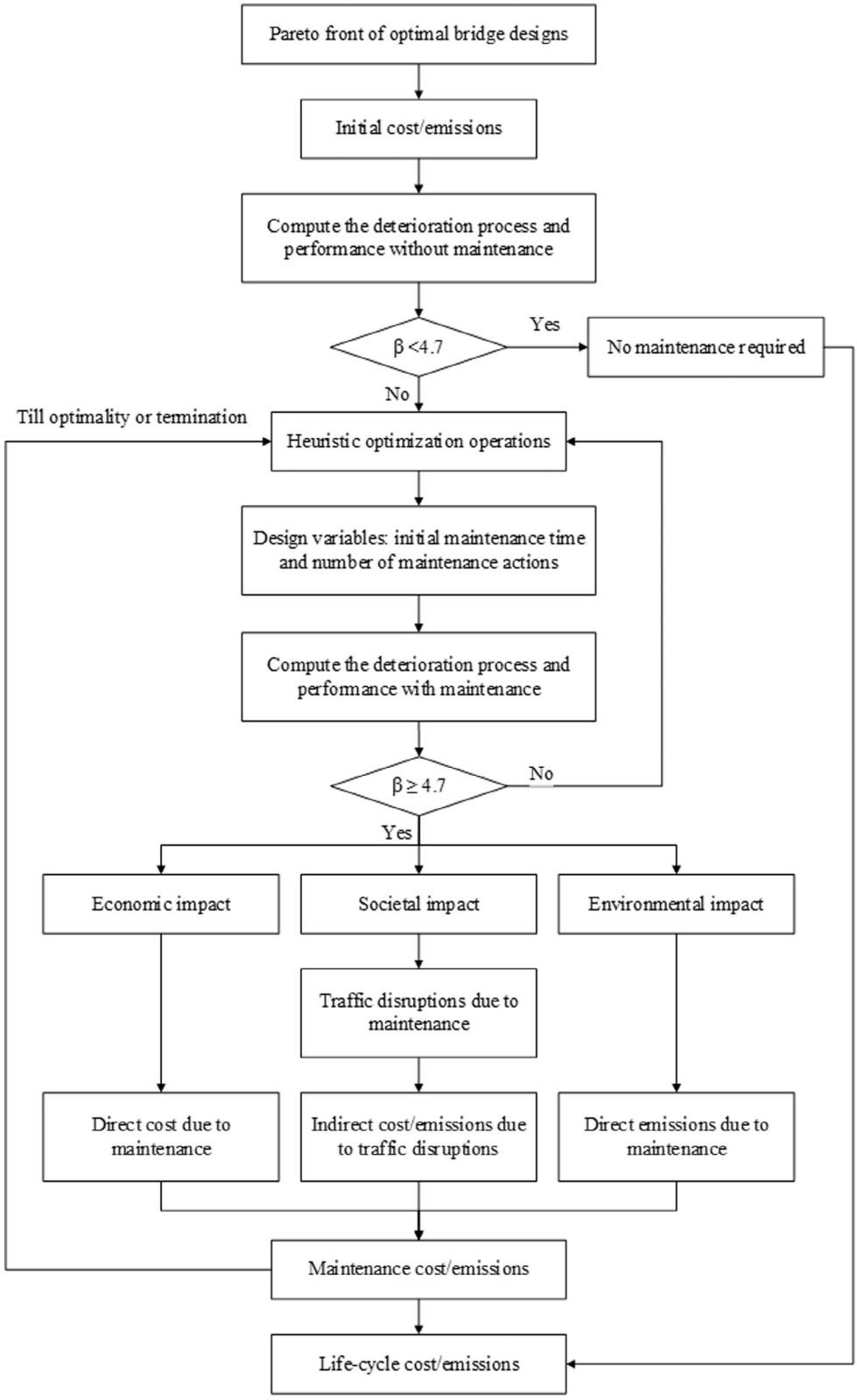

Fig. 3. Flowchart of the optimization procedure.

$$TC = TC_{ms} + C_{ini} \tag{23}$$

$$TE = TE_{ms} + E_{ini} \tag{24}$$

Despite the similarity between cost and emission evaluation, time effects of costs imply different incentives for cost-based and emission-based maintenance optimization. Generally, costs at a later time may suggest less present value considering the discount rate. Thus, there is an incentive to take maintenance actions as late as possible, even though an earlier maintenance action may result in a better structural performance. However, CO_2 emissions are the same irrespective of the time of maintenance actions. To minimize

the emissions, the number of maintenance actions should be the smallest possible. In general, the emission-based optimization favors strategies of earlier maintenance actions, while cost-based optimization gives incentives to postpone the maintenance actions on both surfaces provided that the postpone does not lead to an increase of required maintenance actions.

5. Results

Based on the discussion in Section 2, the Pareto front for initial design optimization is presented in Fig. 4, where nine representative solutions are denoted. These solutions are classified into 3 levels for the overall safety factor and 6 levels for the corrosion initiation time. Regarding the overall safety factor, 1.1 and 1.2 values mark the limits. As for the corrosion initiation time, 15, 30, 45, 60 and 75 years are the boundary markers. Table 8 summarizes the objective values of these nine solutions. The depth (h), the concrete cover (c_c) and the concrete grade (f_{ck}) values are indicated. The amount of reinforcing steel, concrete and prestressing steel per square meter of deck are also shown in Table 8. Solution 9 (S9) presents a corrosion initiation time greater than the service life (150 years). Therefore, this solution does not need any maintenance action. Optimum maintenance actions are examined for the other representative solutions according to the discussion in Section 3.

Fig. 5 shows the time-variant evolution of the reliability index of solution S1 affected by the corrosion of the transverse reinforcement. The smallest reliability index is considered to be the representative value of the entire bridge. In particular, the reliability index regarding the torsion is affected the most by the steel corrosion of transverse reinforcement with respect to surface 2: the reliability index reduces significantly (from 8.6 to 5.5) from t_{corr} to t_2 (year 25). The maintenance application at year 25 delays the deterioration process for about 50 years, which is the time required for the chloride to penetrate through the new concrete cover and to reach the threshold concentration. The longitudinal reinforcement is less affected by the chloride attack since rebars are placed farther away from the surface. Thanks to this increment in concrete cover, the corresponding limit states are not critical for the structural failure. In total, two maintenance actions are required for solution S1 to end the service life with a reliability index greater than 4.7.

Tables 9, 10 and 11 provide the results of cost optimization. Table 9 shows the optimum maintenance plan for the representative solutions. It is worth noting that most of the solutions have simultaneous maintenance actions for surfaces 1 and 2, which can halve the societal impact. The obtained results suggest that, in order to promote sustainability, the number of maintenance actions should be as small as possible to reduce the economic, environmental and societal impacts. It is usually cheaper to reduce the total number of maintenance applications even at the price of advancing the first maintenance date. In addition, it is more sustainable to conduct maintenance activities over all the surfaces at the same time. As the maintenance actions on surfaces 1 and 2 coincide, the societal impact can be greatly reduced. Actually, despite the fact that the costs and CO_2 emissions are optimized separately, both optimizations lead to the same number of maintenance actions, and therefore the same amount of CO_2 emissions. Besides, when fixing this number of maintenance applications and delaying the first maintenance application, the cost is also minimized. Therefore, cost optimization in general can lead to optimal solutions with respect to CO_2 emissions.

The mean values of total life-cycle costs and life-cycle emissions are shown in Tables 10 and 11. The order of the total life-cycle cost from least to greatest is S9, S8, S6, S2, S4, S5, S7, S3 and S1. This order coincides with the corrosion initiation time, with the exception of the solution S4. The findings indicate that the increment in corrosion initiation time reduces the life-cycle cost despite a slight increase in the initial cost. Comparing S4, S5 and S7, solution S4 uses 45 MPa concrete with 3 cm of concrete cover, while the other solutions use 35 MPa and a greater length of concrete cover. As a result, though S4 belongs to a lower level of corrosion initiation time, the increment in concrete strength results in a better life-cycle performance. This result indicates that, for similar corrosion initiation time, increasing the concrete strength may reduce the number of required maintenance actions and, consequently, reduce the life-cycle cost. Therefore, even both the increment in concrete strength and concrete cover results in a better durability level, the increment in concrete strength has better life-cycle results for designs with similar corrosion initiation time. The safety level has less influence on the life-cycle cost. Compared with corrosion initiation time, the safety factor with respect to the critical limit state of the initial design does not necessarily govern the life-cycle reliability level due to different deterioration rates. Consequently, a bridge design with higher initial safety level does not always guarantee a lower life-cycle cost.

Regarding the life-cycle emissions, the order is S9, S2, S6, S8, S5, S7, S3, S1 and S4. In this case, the order does not follow exactly that for the corrosion initiation time. This is because emissions depend only on the total number of maintenance actions regardless of the time of applications. Therefore, solutions with greater corrosion initiation time, which delay the maintenance actions but do not

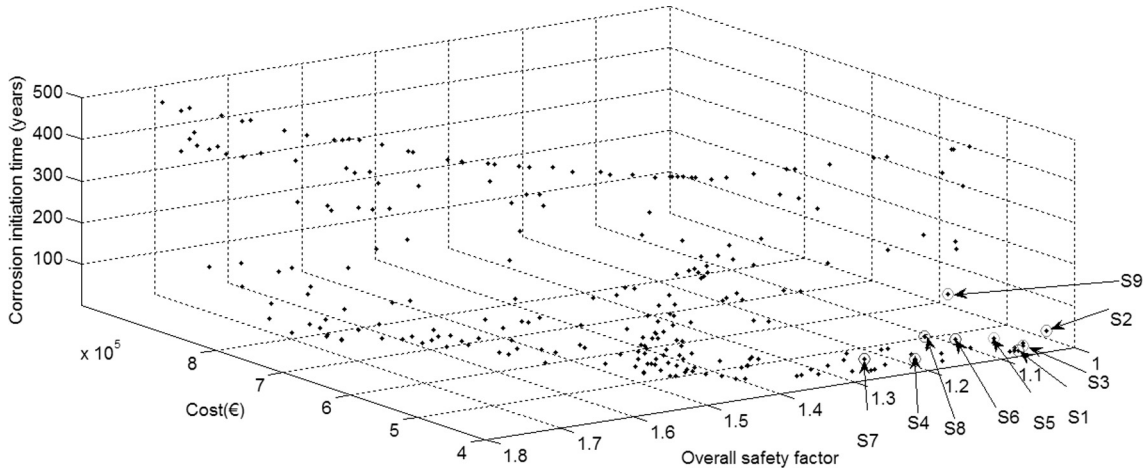

Fig. 4. Representative solutions of the Pareto optimal set.

Table 8
Representative solutions of the Pareto front.

	C_{ini} (€)	S	t_{corr} (years)	h (m)	c_c (m)	f_{ck} (MPa)	Reinforcing steel (kg/m^2 deck)	Concrete (m^3/m^2 deck)	Prestressing steel (kg/m^2 deck)
S1	401260	1.07 (L1)	10.45 (L1)	2.30	0.03	35.00	67.10	0.670	21.99
S2	401400	1.03 (L1)	47.41 (L4)	2.30	0.06	35.00	66.89	0.674	21.98
S3	401950	1.06 (L1)	18.26 (L2)	2.30	0.04	35.00	70.03	0.665	21.11
S4	406160	1.21 (L3)	23.81 (L2)	2.65	0.03	45.00	70.44	0.662	19.80
S5	409810	1.10 (L1)	41.04 (L3)	2.30	0.06	35.00	76.81	0.636	21.10
S6	416610	1.14 (L2)	48.15 (L4)	2.60	0.03	50.00	72.31	0.678	19.80
S7	416830	1.27 (L3)	35.09 (L3)	2.30	0.05	35.00	81.36	0.635	21.10
S8	418640	1.18 (L2)	65.68 (L5)	2.65	0.04	50.00	74.67	0.674	19.80
S9	423570	1.15 (L2)	153.90 (L6)	2.55	0.03	55.00	78.50	0.638	20.46

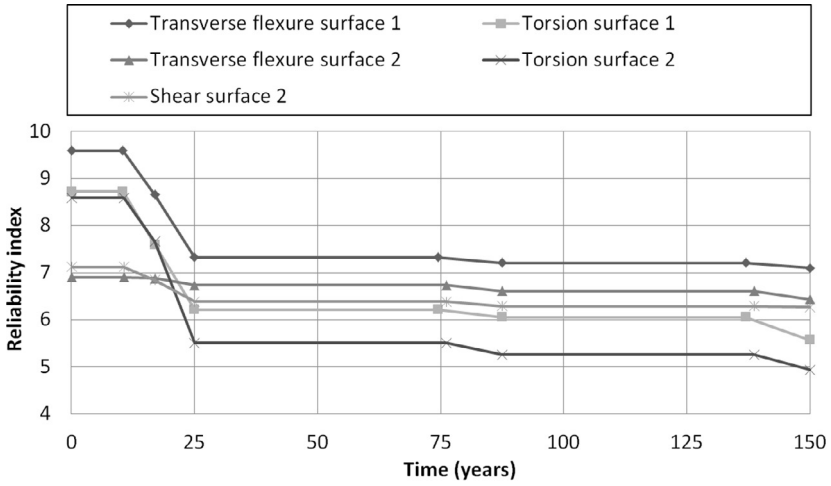

Fig. 5. Reliability index evolution of the limit states affected by maintenance application.

Table 9
Maintenance plan corresponding to the eight representative solutions.

	TC (€)	TE (kg CO_2)	t_1 (years)	n_1	t_2 (years)	n_2
S1	813350	1453090	25	2	25	2
S2	532290	1097020	70	1	70	1
S3	743010	1449710	35	2	35	2
S4	619800	1496230	65	2	65	2
S5	621560	1325940	60	1	60	2
S6	485020	1163320	105	1	105	1
S7	663940	1334580	50	1	50	2
S8	468840	1170620	120	1	120	1

Table 10
Mean life-cycle costs.

	C_{ms1} (€)	C_{ms2} (€)	C_{run} (€)	C_{time} (€)	C_{ini} (€)	TC (€)
S1	134628	107392	11045	66598	400966	813350
	39051	31148	3204	19318		
S2	55209	44037	4527	27264	401250	532290
S3	116330	78369	9046	54643	401870	743010
	37251	25098	2897	17499		
S4	53809	60348	5007	30085	406220	619800
	23192	26011	2158	12967		
S5	76256	56918	5534.9	33310	410260	621560
		23347	2270.4	13664		
S6	24413	27748	2271	13704	416886	485020
S7	92540	65389	6753	40347	417120	663940
		24294	2509	14990		
S8	18077	20276	1681	10153	418650	468840
S9					425710	425710

Table 11
Mean life-cycle emissions.

	E_{ms1} (kg CO_2)	E_{ms2} (kg CO_2)	E_{run} (kg CO_2)	E_{ini} (kg CO_2)	TE (kg CO_2)
S1	170832	141393	44969	738705	1453090
	170832	141393	44969		
S2	171045	141564	44904	739510	1097020
S3	177518	130747	44938	743308	1449710
	177518	130747	44938		
S4	145803	175193	45038	764160	1496230
	145803	175193	45038		
S5	185880	146132	44841	758113	1325940
		146132	44841		
S6	145951	177822	44997	794550	1163320
S7	185963	141371	44997	775843	1334580
		141371	45030		
S8	146359	175847	44963	803446	1170620
S9				817970	817970

eliminate it, are not effective from the environmental point of view.

6. Conclusions

This paper compares the life-cycle performance of a set of alternative tradeoff solutions of a bridge design. A continuous PTC box-girder road bridge located in a coastal region is studied. The bridge is optimized in terms of cost, corrosion initiation time and structural safety. The effect of the objectives on the life-cycle performance regarding the sustainable goal is examined. The chloride-induced corrosion deteriorates the reinforcing steel and decreases the structural capacity. The optimum sustainable maintenance is obtained to maintain the reliability of the structure over the threshold during the service life. The economic, environmental and societal impacts of bridge maintenance actions are minimized. The economic impact considers the cost of direct maintenance. The environmental impact evaluates the CO_2 emissions due to maintenance. The impact of traffic disruptions on the society is computed in terms of cost and CO_2 emissions. The following conclusions can be drawn from this paper:

- The time of initial maintenance application and the number of maintenance actions control the deterioration of structural performance and the economic, environmental and societal impacts. The time of initial application influences the present cost when considering the discount rate. Maintenance actions that take place earlier result in a better structural performance but at a greater cost.
- The time of application has no influence on the environmental impact. Therefore, the strategy to minimize the maintenance emissions consists of reducing the number of maintenance actions.
- Generally, cost optimization also results in CO_2 emission minimization. This is because, similar to emission minimization, cost objective seeks to reduce the total number of maintenance applications. However, cost optimization has an additional incentive to delay the first application date.
- The deterioration of different surfaces is independent to each other due to their different deterioration conditions. Nevertheless, results in this paper recommend not to adjust the optimum maintenance over each surface separately. Maintenance actions should be scheduled at the same time to reduce the impact of traffic disruptions imposed on society.
- Limit states affected by the corrosion of the transverse reinforcing are more critical than the limit states associated with the longitudinal reinforcing. Results show that the time-variant reliability must be studied over each limit state, since the initial critical limit state may no longer be of relevance when deterioration is considered.
- Findings indicate that it is advisable to improve the durability during the bridge design by increasing the corrosion initiation time. This approach increases the initial cost but decreases the life-cycle cost. However, a higher initial safety level does not always result in a better life-cycle performance. Regarding the durability improvement, the increment in concrete strength can give better life-cycle results when a substantial increase in cover thickness is not possible.

Acknowledgments

The authors acknowledge the financial support of the Spanish Ministry of Economy and Competitiveness, along with FEDER funding (BRIDLIFE Project: BIA2014-56574-R) and the Research and Development Support Program of Universitat Politècnica de València (PAID-02-15).

References

[1] Butlin J. Our common future. By World commission on environment and development. (London, Oxford University Press, 1987, pp.383). J Int Dev 1989;1:284–7. http://dx.doi.org/10.1002/jid.3380010208.
[2] Martí JV, Gonzalez-Vidosa F, Yepes V, Alcalá J. Design of prestressed concrete precast road bridges with hybrid simulated annealing. Eng Struct 2013;48:342–52. http://dx.doi.org/10.1016/j.engstruct.2012.09.014.
[3] Martínez-Martín FJ, González-Vidosa F, Hospitaler A, Yepes V. A parametric study of optimum tall piers for railway bridge viaducts. Struct Eng Mech 2013;45:723–40.
[4] Belevičius R, Jatulis D, Šešok D. Optimization of tall guyed masts using genetic algorithms. Eng Struct 2013;56:239–45. http://dx.doi.org/10.1016/j.engstruct.2013.05.012.
[5] Ahsan R, Rana S, Ghani SN. Cost optimum design of posttensioned I-girder bridge using global optimization algorithm. J Struct Eng 2012;138:273–84. http://dx.doi.org/10.1061/(ASCE)ST.1943-541X.0000458.
[6] García-Segura T, Yepes V, Alcalá J, Pérez-López E. Hybrid harmony search for sustainable design of post-tensioned concrete box-girder pedestrian bridges. Eng Struct 2015;92:112–22. http://dx.doi.org/10.1016/j.engstruct.2015.03.015.
[7] Martí JV, García-Segura T, Yepes V. Structural design of precast-prestressed concrete U-beam road bridges based on embodied energy. J Clean Prod 2016;120:231–40. http://dx.doi.org/10.1016/j.jclepro.2016.02.024.
[8] Yepes V, Martí JV, García-Segura T. Cost and CO2 emission optimization of precast–prestressed concrete U-beam road bridges by a hybrid glowworm swarm algorithm. Autom Constr 2015;49:123–34. http://dx.doi.org/10.1016/j.autcon.2014.10.013.
[9] Park H, Kwon B, Shin Y, Kim Y, Hong T, Choi S. Cost and CO2 emission optimization of steel reinforced concrete columns in high-rise buildings. Energies 2013;6:5609–24. http://dx.doi.org/10.3390/en6115609.
[10] García-Segura T, Yepes V. Multiobjective optimization of post-tensioned concrete box-girder road bridges considering cost, CO2 emissions, and

safety. Eng Struct 2016;125:325–36. http://dx.doi.org/10.1016/j.engstruct.2016.07.012.
[11] García-Segura T, Yepes V, Alcalá J. Life cycle greenhouse gas emissions of blended cement concrete including carbonation and durability. Int J Life Cycle Assess 2014;19:3–12. http://dx.doi.org/10.1007/s11367-013-0614-0.
[12] Collins F. Inclusion of carbonation during the life cycle of built and recycled concrete: influence on their carbon footprint. Int J Life Cycle Assess 2010;15:549–56. http://dx.doi.org/10.1007/s11367-010-0191-4.
[13] Sarma KC, Adeli H. Cost optimization of concrete structures. J Struct Eng 1998;124:570–8. http://dx.doi.org/10.1061/(ASCE)0733-9445(1998) 124:5(570).
[14] Lee K-M, Cho H-N, Cha C-J. Life-cycle cost-effective optimum design of steel bridges considering environmental stressors. Eng Struct 2006;28:1252–65. http://dx.doi.org/10.1016/j.engstruct.2005.12.008.
[15] Kendall A, Keoleian GA, Helfand GE. Integrated life-cycle assessment and life-cycle cost analysis model for concrete bridge deck applications. J Infrastruct Syst 2008;14:214–22. http://dx.doi.org/10.1061/(ASCE)1076-0342(2008) 14:3(214).
[16] Safi M, Sundquist H, Karoumi R. Cost-efficient procurement of bridge infrastructures by incorporating life-cycle cost analysis with bridge management systems. J Bridg Eng 2015;20:4014083. http://dx.doi.org/10.1061/(ASCE)BE.1943-5592.0000673.
[17] Frangopol DM. Life-cycle performance, management, and optimisation of structural systems under uncertainty: accomplishments and challenges. Struct Infrastruct Eng 2011;7:389–413. http://dx.doi.org/10.1080/15732471003594427.
[18] Frangopol DM, Soliman M. Life-cycle of structural systems: recent achievements and future directions. Struct Infrastruct Eng 2016;12:1–20. http://dx.doi.org/10.1080/15732479.2014.999794.
[19] Cheung MM, Zhao J, Chan YB. Service life prediction of RC bridge structures exposed to chloride environments. J Bridg Eng 2009;14:164–78. http://dx.doi.org/10.1061/(ASCE)1084-0702(2009) 14:3(164).
[20] Kim S, Frangopol DM, Soliman M. Generalized probabilistic framework for optimum inspection and maintenance planning. J Struct Eng 2013;139:435–47. http://dx.doi.org/10.1061/(ASCE)ST.1943-541X.0000676.
[21] Neves LC, Frangopol DM. Condition, safety and cost profiles for deteriorating structures with emphasis on bridges. Reliab Eng Syst Saf 2005;89:185–98. http://dx.doi.org/10.1016/j.ress.2004.08.018.
[22] Neves LAC, Frangopol DM, Petcherdchoo A. Probabilistic lifetime-oriented multiobjective optimization of bridge maintenance: combination of maintenance types. J Struct Eng 2006;132:1821–34. http://dx.doi.org/10.1061/(ASCE)0733-9445(2006) 132:11(1821).
[23] Chiu C-K, Lin Y-F. Multi-objective decision-making supporting system of maintenance strategies for deteriorating reinforced concrete buildings. Autom Constr 2014;39:15–31. http://dx.doi.org/10.1016/j.autcon.2013.11.005.
[24] Liu M, Frangopol DM. Multiobjective maintenance planning optimization for deteriorating bridges considering condition, safety, and life-cycle cost. J Struct Eng 2005;131:833–42. http://dx.doi.org/10.1061/(ASCE)0733-9445(2005)131:5(833).
[25] Dong Y, Frangopol DM, Saydam D. Time-variant sustainability assessment of seismically vulnerable bridges subjected to multiple hazards. Earthq Eng Struct Dyn 2013;42:1451–67. http://dx.doi.org/10.1002/eqe.2281.
[26] Sabatino S, Frangopol DM, Dong Y. Sustainability-informed maintenance optimization of highway bridges considering multi-attribute utility and risk attitude. Eng Struct 2015;102:310–21. http://dx.doi.org/10.1016/j.engstruct.2015.07.030.
[27] Penadés-Plà V, García-Segura T, Martí J, Yepes V. A review of multi-criteria decision-making methods applied to the sustainable bridge design. Sustainability 2016;8:1295. http://dx.doi.org/10.3390/su8121295.
[28] Frangopol DM, Kim S. Service life, reliability and maintenance of civil structures. In: Lee LS, Karbari V, editors. Life Estim. Ext. Civ. Eng. Struct.. Elsevier; 2011. p. 145–78. http://dx.doi.org/10.1533/9780857090928.2.145.
[29] Wisniewski DF, Casas JR, Ghosn M. Simplified probabilistic non-linear assessment of existing railway bridges. Struct Infrastruct Eng 2009;5:439–53. http://dx.doi.org/10.1080/15732470701639906.
[30] García-Segura T, Yepes V, Frangopol DM. Multi-objective design of post-tensioned concrete road bridges using artificial neural networks. Struct Multidiscip Optim 2017. doi:10.1007/s00158-017-1653-0.
[31] Fomento M. EHE-08: Code on structural concrete. Madrid, Spain: Ministerio de Fomento; 2008.
[32] Fomento M. IAP-11: Code on the actions for the design of road bridges. Madrid, Spain: Ministerio de Fomento; 2011.
[33] European Committee for Standardisation. EN1992-2:2005. Eurocode 2: Design of concrete structures-Part 2: Concrete Bridge-Design and detailing rules. Brussels; 2005.
[34] European Committee for Standardisation. EN 1991-2:2003. Eurocode 1: Actions on structures-Part 2: Traffic loads bridges; 2003.
[35] Vu KAT, Stewart MG. Structural reliability of concrete bridges including improved chloride-induced corrosion models. Struct Saf 2000;22:313–33. http://dx.doi.org/10.1016/S0167-4730(00)00018-7.
[36] Papadakis VG, Roumeliotis AP, Fardis MN, Vagenas CG. Mathematical modelling of chloride effect on concrete du-rability and protection measures. In: Dhir RK, Jones MR, editors. Concr. repair, Rehabil. Prot.. London: E&FN Spon; 1996. p. 165–74.
[37] McGee R. Modeling of durability performance of Tasmanian bridges. In: Melchers R, M.G S, editors. Appl. Stat. Probab. Civ. Eng. Reliab. risk Anal., Rotterdam: A.A. Balkema; 1999, p. 297–306.
[38] European Committee for Standardisation. EN 1990:2002. Eurocode: Basis of structural design; 2002.
[39] Ellingwood B, Galambos TV, MacGregor JG, Cornell CA. Development of a probability based load criterion for American National Standard A58: building code requirements for minimum design loads in buildings and other structures, vol. 13. U.S. Department of Commerce, National Bureau of Standards; 1980.
[40] Gulvanessian H. SAKO Report. Appendix B - Investigation by BRE (using reliability analysis) of the alternative combination rules provided in EN 1990 "Basis of Structural Design"; 2003.
[41] European Committee for Standardisation. EN 1991-1-5:2003. Eurocode 1: Actions on structures - Part 1–5: General actions – Thermal actions; 2003.
[42] Crespo-Minguillón C, Casas JR. Fatigue reliability analysis of prestressed concrete bridges. J Struct Eng 1998;124:1458–66. http://dx.doi.org/10.1061/(ASCE)0733-9445(1998) 124:12(1458).
[43] Gulvanessian H, Holický M. Reliability based calibration of Eurocodes considering a steel member. Zurich: JCSS Work. Reliab. based code calibration; 2002.
[44] Sanpaolesi L, Croce P. Handbook 4: design of bridges-guide to basis of bridge design related to Eurocodes supplement by practical examples, Bridg. – Actions load Comb., Pisa; 2005.
[45] Bouassida Y, Bouchon E, Crespo P, Croce P, Davaine L, Denton S, et al. Bridge design to Eurocodes-Worked examples. In: Athanasopoulou A, Poljansek M, Pinto A, Tsionis G, Denton S, editors. Work. "Bridge Des. to Eurocodes," Vienna, 4 - 6 Octobe 2010. Luxe mbourg: Publications Office of the European Union; 2010.
[46] Nowak AS. Live load model for highway bridges. Struct Saf 1993;13:53–66. http://dx.doi.org/10.1016/0167-4730(93)90048-6.
[47] Geem ZW, Kim JH, Loganathan GV. A new heuristic optimization algorithm: Harmony search. Simulation 2001;76:60–8.
[48] BEDEC. Institute of Construction Technology of Catalonia. Barcelona, Spain. www.itec.cat (December 10, 2015).
[49] Hidrodemolición. http://www.hidrodemolicion.com/ (December 21, 2015).
[50] DRIZORO S.A.U. Productos para la Construcción. http://www.drizoro.com/ (December 21, 2015).